Positronium as a Probe of Polymer Free Volume

Subjects: Polymer Science

Contributor: Giovanni Consolati , Dario Nichetti , Fiorenza Quasso

Positron annihilation lifetime spectroscopy (PALS) is a valuable technique to investigate defects in solids, such as vacancy clusters and grain boundaries in metals and alloys, as well as lattice imperfections in semiconductors. In the case of polymers, PALS is able to give information on the holes forming the free volume; this quantity, is correlated to important mechanical, thermal, and transport properties of polymers. PALS supplies a quantitative measure of the free volume by probing the corresponding sub-nanometric holes. The system used is positronium (Ps), an unstable atom formed by a positron and an electron, whose lifetime can be related to the typical size of the holes.

free volume | positron annihilation lifetime spectroscopy | polymers | membranes | biopolymers | composites | rubbers

1. Introduction

Although not univocally defined [1], the concept of free volume can be used to explain various features of polymers. For instance, mechanical properties [2] are generally (negatively) correlated to the free volume fraction of the polymer. Indeed, the applied load tends to concentrate in the free volume instead of distributing among the molecules of the polymer, and this can result in the failure of the material. Therefore, a polymer with a reduced free volume fraction generally shows better mechanical properties [3]. Transport properties are of the utmost importance in polymer membranes used in molecular separation processes such as water desalinization or environmental remediation. In this case, too, the free volume holes in the polymer matrix are responsible for gas separation [4][5].

Roughly speaking, the free volume is the difference between the total volume and ‘occupied’ volume. When the occupied volume includes the volume swept out by a molecular segment due to thermal vibration (‘fluctuation volume’ [6]), the difference between the total volume and this ‘vibrational’ volume is excess free volume, which allows movements of polymer segments. Free volume holes refer to this excess free volume, which has been incorporated in some cell models [7].

Holes can be examined by various probes, such as photochromic labels [8], fluorescence molecules [9], or techniques such as small angle XRD [10]. Positron annihilation lifetime spectroscopy (PALS) uses positronium (Ps), a bound electron-positron state, to gain information about the size and distribution of free volume holes (information about the physical properties of Ps can be found in a review by Berko and Pendleton [11]). This non-

destructive technique is based on the fact that Ps is repelled from the molecules of the polymer, due to the exchange repulsion between the Ps electron and surrounding electrons and localizes into the open spaces of the host structure. In this sense it is a ‘seeker’ of free volume holes.

2. Positronium in Polymers

Ps is an unstable system, subjected to annihilation. Para-Ps (p-Ps, antiparallel spins) and ortho-Ps (o-Ps, parallel spins) are the two sublevels of ground state Ps, characterized by the different spin orientation of the two particles [12]. In a vacuum, p-Ps has a lifetime of 125 ps; o-Ps lifetime is much longer, 142 ns. In a material, p-Ps is scarcely influenced by the environment and changes in its lifetime are small; on the other hand, in a hole, o-Ps undergoes interactions with surrounding electrons and o-Ps can annihilate, in addition with its own electron, also with an outer electron in relative singlet spin state. This ‘pickoff’ process is responsible for the decrease in o-Ps lifetime with respect to its value in a vacuum up to two orders of magnitude, depending on the overlap between the wave functions of the positron and surrounding electrons [13].

The free volume hole size can be estimated from o-Ps lifetime as supplied by the experiment; to this purpose holes have to be modeled within a suitable geometry. The most popular model for polymers is the spherical one [14][15], although other geometries have been applied.

Tao [14] and later Eldrup [15] found a relationship between o-Ps lifetime and the size of the cavity hosting Ps. Their model assumes a spherical void with effective radius R. This Ps trap has a potential well with finite depth; however, for convenience of calculation, an infinite depth is assumed, with a corresponding increase in the radius to $R + \Delta R$, ΔR being an empirical parameter [16] that describes the penetration of the Ps wave function into the bulk.

The relationship between pickoff decay rate and radius of the hole is:

$$\lambda_p = \lambda_0 \left[\frac{\Delta R}{R + \Delta R} + \frac{1}{2\pi} sin\left(2\pi \frac{R}{R + \Delta R} \right) \right] \quad (1)$$

The o-Ps lifetime τ_3 as determined by the experiment is the reciprocal of the pickoff decay rate, in a very good approximation.

Another parameter available from PALS measurements is o-Ps intensity I_3, the normalized amount of o-Ps in the positron annihilation lifetime spectrum. It is usually related to the number density of holes, N, assuming a linear relation between N and o-Ps intensity I_3 [17]:

$$f = CI_3 v_h \quad (2)$$

where v_h is the volume of the spherical hole as obtained by o-Ps lifetime using the Tao-Eldrup Equation (1) and C is a structural constant. Often a relative free volume, $I_3 v_h$, is used in the discussion of the results.

In the following Table 1 lifetimes and intensities of some polymers are shown, together with the corresponding sizes of free volume holes, in spherical approximation. Sometimes, two long components corresponding to Ps in bigger and smaller holes are found.

Table 1. Ps lifetime and intensity of some polymers. The radius of the spherical hole is also shown. LDPE: low density polyethylene, HDPE: high density polyethylene, PMMA: poly (methyl methacrylate), PET: poly (ethylene terephthalate), SBR: styrene/butadiene rubber, PTFE: poly tetrafluoroethylene, PDMS: polydimethylsiloxane, PTMSP: poly [1-(trimethyl-silyl)propine].

Polymer	τ_3 (ns)	R_3 (nm)	I_3 (%)	τ_4 (ns)	R_4 (nm)	I_4 (%)	Ref.
LDPE	2.55 ± 0.01	0.33	21.1 ± 0.4				[18]
HDPE	2.38 ± 0.04	0.32	19.7 ± 0.3				[19]
Nylon-6	1.55 ± 0.02	0.24	24.5 ± 0.04				[20]
PMMA	1.92 ± 0.01	0.28	23.6 ± 0.02				[21]
PET	1.66 ± 0.03	0.25	20.4 ± 0.3				[22]
Cis1,4-polybutadiene	2.614 ± 0.005	0.34	39.45 ± 0.07				[23]
SBR	2.50 ± 0.02	0.33	34.2 ± 0.9				[24]
PDMS	3.27 ± 0.03	0.39	30.3 ± 0.5				[25]
Nafion	3.27 ± 0.01	0.39	6.33 ± 0.06				[26]
PTFE	1.12 ± 0.09	0.19	9.6 ± 0.9	3.92 ± 0.02	0.43	13.8 ± 0.2	[27]
PTMSP	4.7 ± 0.3	0.47	9.7 ± 0.5	13.8 ± 0.1	0.79	31.1 ± 0.6	[28]

3. Experimental Setup

In most of the studies of bulk polymers, positrons are generated from the decay of ^{22}Na, a nuclide emitting a positron and, almost simultaneously, a γ-ray whose energy is 1.27 MeV. This ‘start’ photon signals the birth of the positron. The ‘stop’ signal is provided by one of the annihilation photons: most of the annihilations ordinarily occur into two γ-rays (0.51 MeV each). The source (whose activity is often in the range 0.04 to 1 MBq) is prepared by depositing a droplet of an aqueous solution containing ^{22}Na on a thin metallic or plastic foil; after drying, it is covered by an identical support and sealed, to obtain a source that can be used several times.

Figure 1 is a sketch of a PALS timing spectrometer [29], showing two channels: each one consists of a scintillator coupled to a photomultiplier tube (PMT). The scintillator converts the γ-rays into UV-vis photons, which when hitting the PMT photocathode generate photoelectrons. A constant fraction discriminator (CFD) on each channel generates a fast-timing signal whenever a γ-ray with the correct energy is detected. A time-to-amplitude converter (TAC) activated by the start CFD produces a voltage proportional to the lifespan of the positron. This signal, digitized by an analog-to-digital converter (ADC), is transferred to a personal computer (PC).

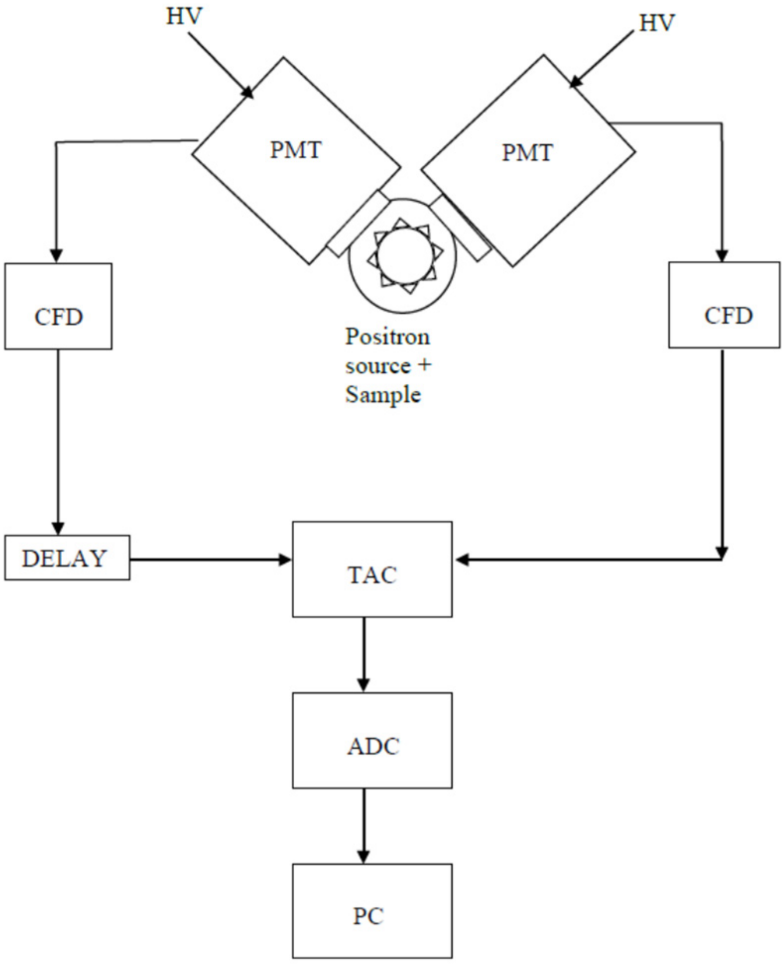

Figure 1. A PALS spectrometer.

Starting from 2000, signals from the PMT can also be digitized by means of ultra-fast modules, replacing some of the units (CFD and TAC) of the apparatus [30][31]. Digitized pulses stored in a personal computer can be analyzed off-line; digital filters select pulses with suitable shape and amplitude. Time resolution is improved with respect to the standard configuration, without decreasing the counting rate [32]. The introduction of ultra-fast digitizers has represented a real milestone in the PALS technique [33][34][35].

The annihilation lifetime spectrum is a histogram (with a statistic of one to several millions of counts), which can be analyzed by means of a suitable computer code.

Several computer programs have been published and made available [36][37][38][39] to analyze the annihilation lifetime spectrum. A PALS spectrum consists of the sum of a number of components, each corresponding to a particular positron state, considered as *discrete* and/or *continuous*. In the first case, a component is an exponential function of the form , characterized by a lifetime τ and intensity I. A value around 0.4 ns is typical for lifetimes of free positrons (*i.e.*, not forming Ps) in polymers. p-Ps lifetimes in condensed matter are generally within 0.15 ns; o-Ps shows the longest lifetimes, typically in the range 1–10 ns. Sometimes two long components are found in polymer spectra (see **Table 1**).

A continuous PALS component is built as a continuous sum of discrete components. Three parameters describe it: the intensity and first two moments of the distribution of lifetimes: centroid and standard deviation from the mean lifetime. A distribution of o-Ps lifetimes (sometimes two distributions) can be expected in a polymeric material, reflecting the hole volume distribution present in the amorphous zones.

In order to resolve the continuous components of a spectrum with good accuracy, statistics should be higher than a discrete analysis.

4. Discussion of Some Positron Annihilation Lifetime Spectroscopy Results in Polymeric Systems

Only a few examples are discussed, to highlight the connection between Ps parameters and free volume. A more complete discussion can be found in ref. [40].

4.1. Membranes

Membranes are the subject of a large number of investigations, due to the obvious interest in many fields. PALS has been applied to different membranes. Considering proton exchange membranes, hybrid Nafion membranes were investigated at different humidities [41]. o-Ps lifetime is associated with the microstructure evolution and the development of hydrophilic ion clusters as a function of water uptake. The maximum value of o-Ps lifetime corresponds to the formation of numerous water channels for proton transportation, suggesting that transportation of protons can be more efficient at lower relative humidity.

Another investigation concerning two commercial Nafion membranes [42] revealed a good correlation between the size of free volume holes as obtained from PALS and proton conductivity, showing that this last is essentially governed by the free volume present in the polymer.

In another study on three commercial per-fluorinated sulfonic acid/PTFE proton exchange membranes [43], o-Ps lifetime was studied as a function of time at 70% RH and versus RH, in both cases at room temperature. o-Ps lifetime increases with time, leveling off after about 60 h, which is explained in terms of accumulation of water molecules inside the membranes, whose nanostructure is stabilized preventing further change of the hole volume. The behavior of o-Ps lifetime with RH is non-monotonous (**Figure 2**): by increasing RH, lifetime first decreases due

to the filling of hole volumes by water molecules. Then, o-Ps lifetime begins to increase, due to membrane plasticization induced by higher water content, which involves an increased hole volume.

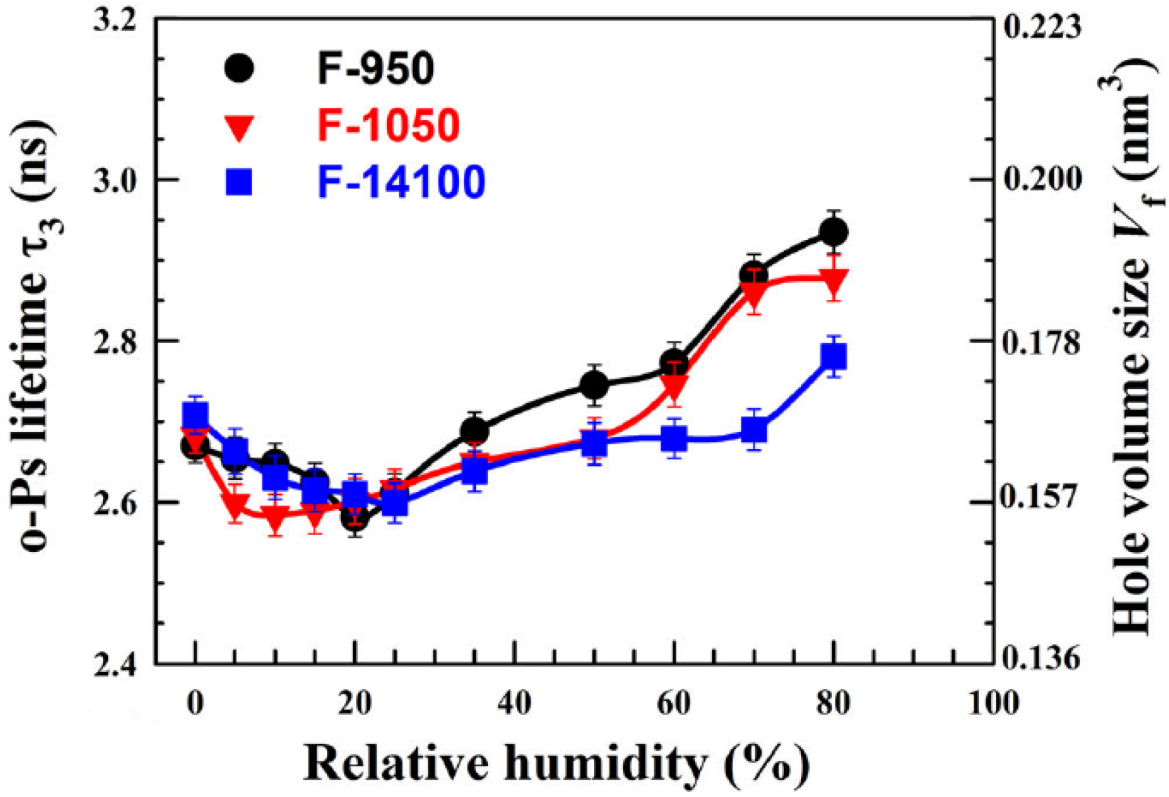

Figure 2. Variation of the o-Ps lifetime as a function of RH for the three investigated membranes. The right *y* axis represents the hole volume size as derived from the Tao-Eldrup model (reproduced from ref. [43] with permission from John Wiley & Sons. DOI: 10.1002/pat5570).

Free volume as determined by PALS in crosslinked PVA/SSA proton exchange membranes with different concentration of sulfosuccinic acid (SSA) [44] supplies a microscopic interpretation of the tensile strength versus the SSA content, which decreases above 15 wt%. Indeed, o-Ps lifetime increases when SSA content > 15 wt%: bigger free volume holes reduce the interactions among the polymer segments, and the corresponding higher chain mobility gives flexibility to the structure, decreasing the tensile strength.

4.2. Composites

Polymer composites are an active research field. PVA-PVP blends were investigated at increasing loading of magnesia, 0.5 up to 2 wt% [45]. o-Ps lifetime is found to decrease with loading magnesia, while intensity remains almost constant. On the whole, the relative fractional free volume, $v_h I_3$ decreases, which is interpreted in terms of partially filling the holes in the blend matrix by the magnesia nanoribbons. This is confirmed by a linear relationship between the hole volume and equilibrium swelling ratio, ESR.

A study on PDMS filled by fumed silica (FS) was undertaken [46], in order to understand the mechanism of water diffusion after corona discharge, a proxy of the failure of this composite used as insulating material in power grids. A different behavior of o-Ps lifetime was found by increasing the FS content: above about 6% the lifetime, which is stable for lower values, linearly decreases, due to a change from a dispersed to a percolated state of the FS in the composite: particles are no longer randomly distributed but tightly packed to the matrix. In this case, the overlapping of FS/PDMS interfaces (which represent extra channels for o-Ps trapping, in addition to the free volume holes) supply continuous diffusion paths for water. This provides a microscopic interpretation of the failure mechanism.

A carbon fiber reinforced polymer consisting of a bisphenol-A epoxy resin and PAN-based carbon fibers were investigated by PALS and X-ray computed tomography [47]. Crack initiation and propagation in the sample was observed by in situ measurements of X-CT during a tensile test. Analysis of o-Ps lifetimes revealed cavities greater than those found in the polymer matrix not subjected to testing and associated to breaks in the molecular chains upon fracture and formed from an agglomeration of holes.

A nanocomposite is a hybrid system with a polymer matrix and filler composed by nanoparticles. A huge number of nanofillers is used, e.g., based on carbon, silica, or metals. Complex and interesting features concern the free volume in the polymeric matrix of the nanocomposite. In fact, while various investigations have shown a decrease in the free volume when the matrix incorporates the nanoparticles (e.g., [48][49][50][51]), in other studies [52][53][54], the free volume increases with the concentration of nanofiller, which has been correlated to a weak interaction between the matrix and the filler, favoring the creation of large free volume holes. On the other hand, an interfacial interaction between polymer matrix and nanofiller sufficiently strong to prevail on the interactions among nanoparticles improves the dispersion of nanofiller in the matrix, with a consequent reduction of free volume. In these cases, an improvement of the tensile properties of the nanocomposite is observed, as it can be expected.

An exhaustive review of PALS studies in nanocomposites can be found in ref. [55].

4.3. Porous Polymers

Micro and mesopores present in polymer networks are studied through gas absorption; comparison with PALS reveals interesting features. For instance, in a series of amorphous melamine-based polymers [56] both PALS and N_2 absorption isotherms show the same kind of voids; however, PALS gives the correct micropore volume, which is underestimated by the other classical method.

Micropores distributions in different amorphous polymer glasses have also been investigated [57] using low-temperature CO_2 gas sorption and PALS. Two o-Ps lifetimes are found and the corresponding effective sizes of the nanopores are very near to the maxima of the distributions found by the sorption technique (**Figure 3**). Thus, PALS can be a useful tool to study the porosity in amorphous polymers, although limited to microporosity, changes in meso pores (due to e.g., supercritical CO_2 or aging) being hardly detectable.

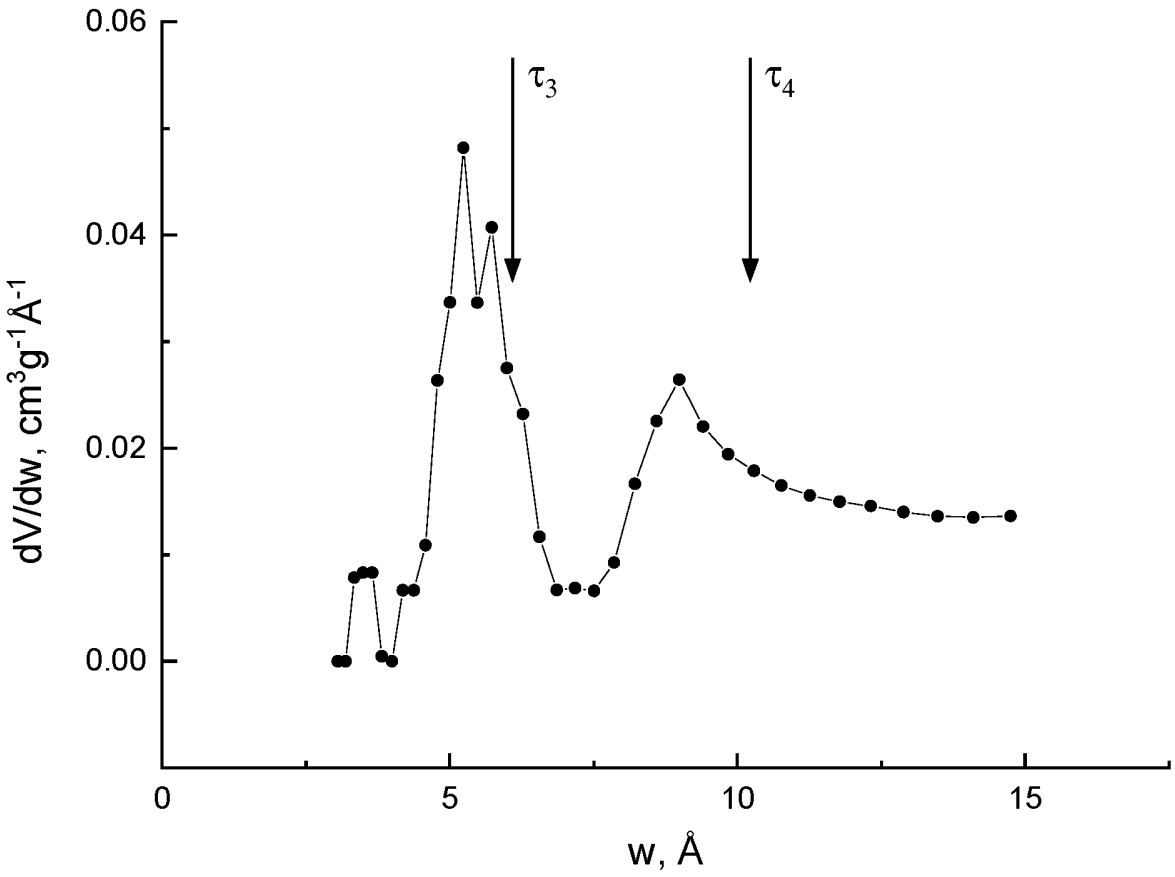

Figure 3. Pore size distribution obtained for a polymer with intrinsic microporosity by the sorption technique with processing, according to the density functional theory NLDFT (*w*: hole size). The vertical arrows indicate the positions of the maxima in the pore size distribution dV/d*w*, according to the positron annihilation data (courtesy by prof. Victor Shantarovich).

The microscopic structure of PVA intercalated montmorillonite was studied by Zhao et al. [58]. o-Ps atoms, distributed between the interlayer spacing of MMT as well as in the free volumes of PVA, show a decreasing lifetime as more PVA chains (up to 20%) are intercalated into MMT layers. At higher PVA loading, an increase in lifetime is observed, interpreted in terms of the presence of micro defects in the exfoliated MMT, since the interlayer space of the exfoliated structure is higher than that in the intercalated structure. This reserach points out the great sensitivity of the PALS technique in highlighting variations in the sizes of micro-defects well below the tenth of nm.

4.4. Bioplastics and Natural Polymers

The importance of natural polymers and bioplastics does not need to be emphasized. Various studies used PALS, combined with other techniques. An investigation concerning the release of a bioactive compound (curcumin) by biopolymers (carrageenan and chitosan) and bioplastics (PLA and poly (butylene adipate-co-terephthalate)) [59] pointed out the role of the free volume. Indeed, a negative correlation has been shown between the release of curcumin and free volume fraction.

Structural changes in a chitosan matrix induced by absorption of two metal ions (Cu (II) and Cr (VI)) were studied using various techniques [60]. o-Ps lifetime is higher in the chitosan matrix than in the samples containing metal ions. The decrease is linear at increasing concentration of Cu, while a strong decrease is observed at low concentrations (<0.38 mM) for the Cr-absorbed samples, which becomes smaller at high concentrations. The results point out that the type of absorbed ion influences the bio matrix more than its concentration, due to the different chitosan-ion interactions: via amino groups in the case of Cu (II), and via both amino and hydroxyl groups in the case of Cr (VI), with a consequent more marked reduction of the free volume holes.

A study involving cellulose was undertaken by Nuruddin et al. [61]. The authors prepared chiral nematic and shear oriented cellulose nanocrystal films, with the aim to find a possible relationship between free volume and gas barrier performance. Their results show that sheared films have lower free volume and exhibit higher tortuosity than chiral nematic self-assembled films, which hinders the diffusion of gases throughout the films. Cellulose nanocrystal films show a higher barrier performance than high barrier polymer films like poly-vinyl alcohol and ethylene vinyl alcohol.

4.5. Coupling PALS and Dilatometry: An Alternative Route to the Free Volume Fraction

Use of Equation (2) to quantify the free volume fraction is common in many studies but should be cautiously considered. In fact, Ps formation and, consequently, I_3 is influenced by various factors [62][63][64], and it is not easy to disentangle the contribution of the number density of holes. In particular, o-Ps intensity in PVAc samples [63] subjected to wide range of temperatures shows hysteresis. The effect has been explained in terms of radiation chemistry processes in the terminal track of the positron [65], and in this case, I_3 cannot be simply correlated to the variation in the number density of holes with temperature. Generally, Ps intensity is often the result of various complicated and interrelated processes [66].

Accordingly, researchers use a different approach, introduced by Srithawatpong et al. [67] and followed also by other authors [68]. The free volume fraction *f* is:

$$f = \frac{N v_h}{V_{sp}} \quad (3)$$

N is the number density of holes and V_{sp} is the specific volume, that is, the sum of free volume and the (specific) occupied volume:

$$V_{sp} = N v_h + V_{occ} \quad (4)$$

where V_{occ} is defined in terms of the Van der Waals volume and the interstitial free volume [68]: $V_{occ} = V_{VdW} + V_{if}$. This latter consists of local voids too minute to host even a small probe such as Ps and it is associated with the occupied volume. The dependence of the occupied volume on the temperature is ascribed to the expansion of such interstitial free volumes and incorporated in the lattice-hole model [69]. In Equations (3) and (4), v_h is the average volume of the holes.

It is possible to obtain N by combining PALS with dilatometry, which supplies the specific volume versus temperature (our investigations were carried out at atmospheric pressure), while from PALS researchers get the average volume of the hole as a function of the temperature, too. Therefore, by plotting V_{sp} versus v_h (both evaluated at the same temperature), N is the slope (at any temperature) of the curve interpolating the experimental data. If both V_{sp} and v_h are linear with temperature, N = const. An example is given in **Figure 4**.

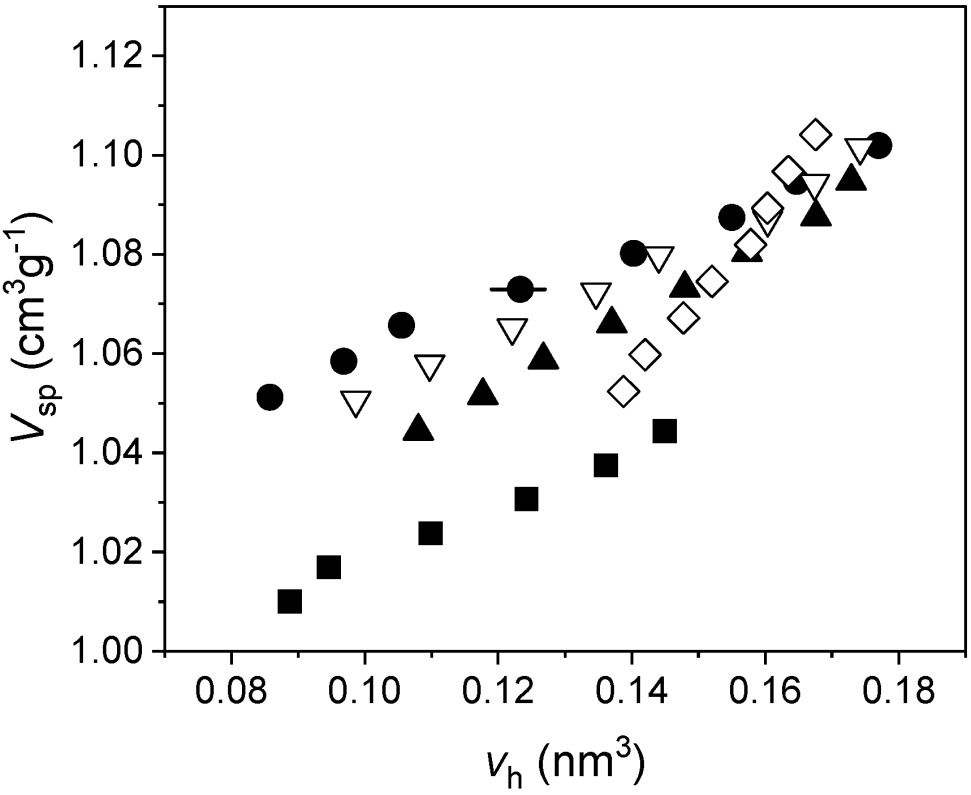

Figure 4. V_{sp} versus v_h, using spherical approximation for the holes, in five different polybutadiene-polyisoprene rubbers. Uncertainties for V_{sp} are within the size of the data, for v_h are shown for a single data point for the sake of clarity (reproduced from ref. [70]. DOI: 10.1002/pi.6431).

By assuming different guesses for the shape of the holes, researchers get different values of v_h at a given temperature, and therefore N is dependent on the choice of the geometry for the cavity. This also influences the values of f, which can be compared to the free volume fraction h, as supplied by the theory, for instance the Simha-Somcynsky equation of state of polymers. Since this last is valid for amorphous polymers at equilibrium, researchers restricted researchers' investigations to temperatures above the glass transition, although it is possible to also extend the theory in the glassy state [71]. Researchers explored polystyrene with different molecular weight

[72], perfluoropolyethers and polypropylene glycols with low molecular weights [73][74], atactic polypropylene [75], polyvinyl acetate [76], a thermoplastic polyurethane [77], and different rubber blends [70][78][79]. Researchers' goal was to explore a possible influence of the investigated structure on the free volume. Researchers adopted a cylindrical geometry for the holes [80], in order to make a comparison with spheres. For a given aspect ratio of the cylinder a different value of the hole volume is obtained, for the same o-Ps lifetime. As a consequence, *f* changes, too, according to Equation (3). Using a least square procedure between *f* and *h* researchers found, for each investigated polymer, the cylindrical cavity which produced the best fit. In most of researchers' investigated polymers the spherical shape is less suitable to describe the free volume holes than cylindrical cavities. In particular, for polystyrenes [72] and polyvinyl acetate [76], researchers found flattened holes. Similar findings were found in various elastomers [70][78][79].

However, the same procedure mentioned above, as applied to polybutadiene-polyisoprene blends [70] and acrylonitrile-butadiene rubbers [79], as well as a terpolymer acrylonitrile-polybutadiene-polyisoprene [79], did not produce satisfactory fits, for any geometrical choice of the cavity.

Anyway, researchers found that the expansion of the holes with temperature seems to proceed anisotropically, being easier in some directions than in others. In other terms, the agreement between *f* and *h* is very good under the guess that the cylinder representing the cavity has a non-linear dependence of the height *s* with the radius *r*:

$$\frac{s}{s_0} = \left(\frac{r}{r_0}\right)^p \quad (5)$$

s_0 and r_0 being height and radius at a given temperature. *p* can be assumed as an index of anisotropic growth: for a cylinder expanding isotropically with temperature *p* = 1. In particular, in polybutadiene-polyisoprene blends researchers found that *p* decreases almost linearly with the content of polyisoprene volume fraction (**Figure 5**), while the presence of acrylonitrile in acrylonitrile-butadiene blends does not change, within the errors, the value of *p* found for pure butadiene.

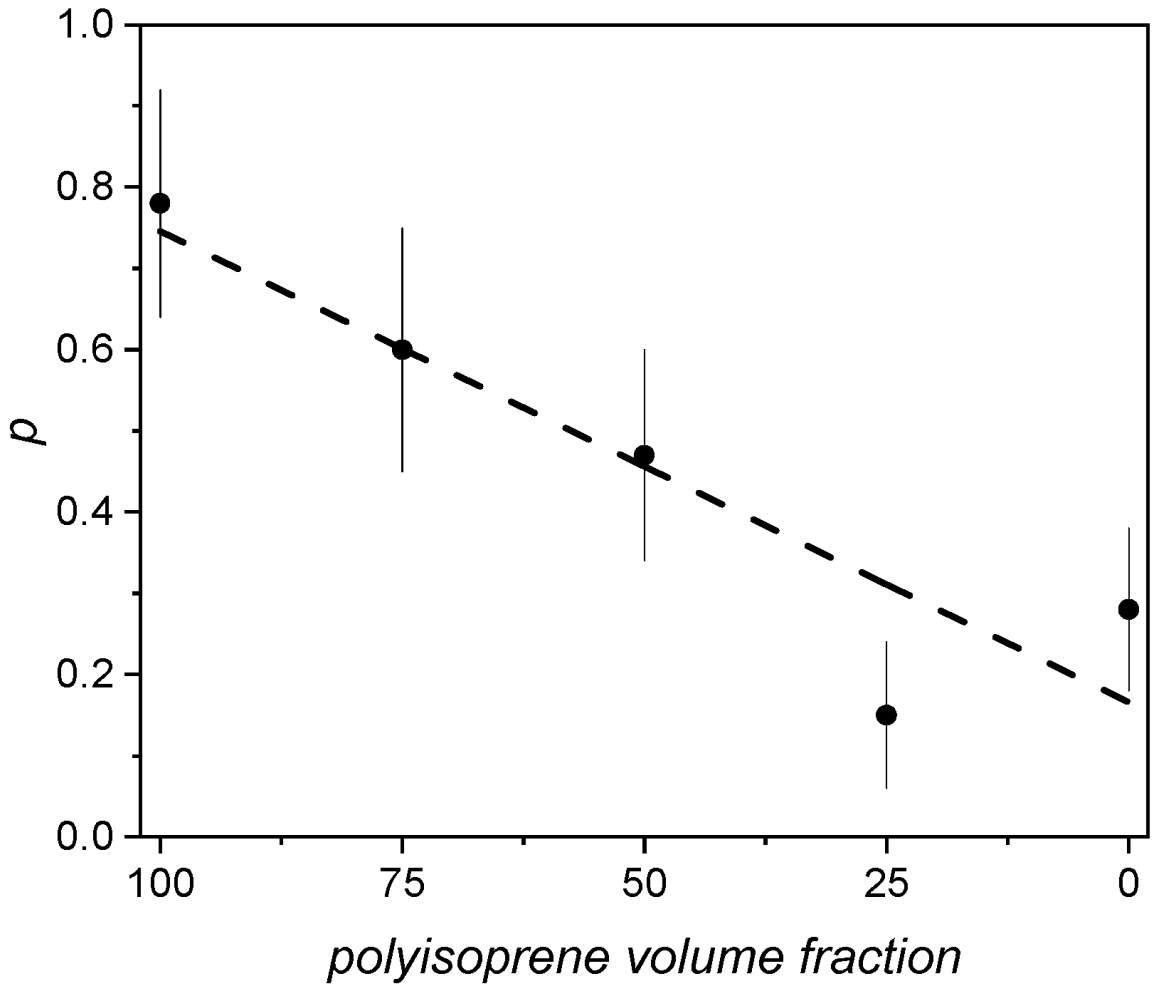

Figure 5. Behavior of parameter *p* versus polyisoprene volume fraction in polybutadiene–polyisoprene blends (reproduced from ref. [79]. DOI: 10.1002/pi.6431).

An analogous anisotropic expansion of the holes was also found for two classes of oligomers: perfluoropolyethers [73] and polypropylene glycols [74].

The anisotropic expansion of the holes, although obtained with a simplified shape, is not in contrast with the presence of physical or chemical constraints (e.g., entanglements or crosslinks), which may hinder the macromolecular motions in some particular directions.

Another result has been found in the three investigated butadiene-acrylonitrile rubbers and the terpolymer polyisoprene-polybutadiene-acrylonitrile [79], extrapolating the hole sizes at the glass transition: they are found in the range 0.6–0.7 nm. These values are comparable to the effective bond length *l*, defined as the square root of the ratio between the unperturbed mean-square end-to-end distance $\langle R^2 \rangle_0$ of a chain and the number of its backbone bonds, which results in 0.5± 0.2 nm, according to Wang [81]. A similar value (0.6 nm) is given by Miller [82]. Researchers found analogous results for a fluoroelastomer, a cis-polyisoprene rubber [78], atactic polypropylene [75], and perfluoropolyethers [73]. It is impressive this remarkable similarity between a typical size of

holes at the glass transition for different polymers and the effective bond length, a parameter related to repetition motions and independent of the macromolecular structure.

5. Conclusions

PALS is a valuable technique to investigate the intra- and inter-chain spaces in polymers, with the unique capability to probe holes with sub-nanometric sizes. In the above discussed examples, researchers tried to point out the importance of this experimental technique that gives a microscopic interpretation of the free volume, a concept related to different macroscopic properties of the material.

A combination of PALS and dilatometry results, integrated with the prediction of the Simha-Somcynsky theory, can give insight on the shape of the free volume holes. Although real holes are irregularly shaped, in some cases a flattened geometry allows one to get better agreement with the theoretical free volume fraction. Furthermore, the growth of the free volume holes with temperature in some polymers seems to be not isotropic, but the expansion appears to be easier in some directions. This sounds reasonable, when researchers consider that the segmental motions of the polymer chains may be hindered by constraints of various kinds.

In conclusion, any advance in the PALS technique, both in the apparatus and data analysis, will allow a more complete view of the free volume fraction, a valuable quantity to explain many polymer properties, but which cannot be measured with macroscopic techniques in a direct way.

References

1. Roe, R.J.; Song, H.H. Isothermal relaxation of volume and density fluctuations of polystyrene glass prepared under pressure. *Macromolecules* **1985**, *18*, 1603.
2. White, R.P.; Lipson, J.L.G. Polymer Free Volume and Its Connection to Glass Transition. *Macromolecules* **2016**, *49*, 3987–4007.
3. Zhang, H.J.; Sellaiyan, S.; Kakizaki, T.; Uedono, A.; Taniguchi, Y.; Hayashi, K Effect of Free-Volume Holes on Dynamic Mechanical Properties of Epoxy Resins for Carbon-Fiber-Reinforced Polymers. *Macromolecules* **2017**, *50*, 3933–3942.
4. Mallon, P.E. Application to polymers.; In Principles and Applications of Positron and Positronium Chemistry; Jean, Y.C., Mallon, P.E., Schrader, D.M., Eds., Eds.; World Scientific: London, UK; pp. 2003; pp. 253–280.
5. Sharma, J.; Tewari, K.; Arya, R.K Diffusion in polymeric systems. A review on free volume theory. . *Prog. Organ. Coat* **2017**, *111*, 83–92.

6. Merkel, T.C.; Freeman, B.D.; Spontak, R.J.; He, Z.; Pinnau, I.; Meakin, P.; Hill, A.J Sorption, transport, and structural evidence for enhanced free volume in poly(4-methyl-2-penthyne)/fumed silica nanocomposite membranes.. *Chem. Mater.* **2003**, *15*, 109–123.
7. Bondi, A. Free Volumes and free rotation in simple liquids and liquid saturated hydrocarbons.. *J. Phys. Chem.* **1954**, *58*, 929.
8. Simha, R.; Somcynsky, T On the statistical thermodynamics of spherical and chain molecules fluids. *Macromolecules* **1969**, *2*, 342.
9. Lamarre, L.; Sung, C.S.P. Studies of physical aging and molecular motion by azochromophoric labels attached to the main chains of amorphous polymers. *Studies of physical aging and molecular motion by azochromophoric labels attached to the main chains of amorphous polymers* **1983**, *16*, 1729.
10. Victor, J.G.; Torkelson, J.M. On measuring the distribution of local free volume in glassy polymers by photochromic and fluorescence techniques. *Macromolecules* **1987**, *20*, 2241.
11. Berko, S.; Pendleton, H.N. Positronium. *Ann. Rev. Nucl. Part. Sci* **1980**, *30*, 543–581.
12. Charlton, M.; Humberston, J.M. Positron Physics; Cambridge Monographs on atomic, molecular and chemical physics: 11. Cambridge University Press, United Kingdom, 2001; ch. 1.
13. Jean, Y.C. Characterizing free volumes and holes in polymers by positron annihilation spectroscopy. In Positron Spectroscopy of Solids; Dupasquier, A., Mills, A.P., Jr., Eds.; IOS Press: Amsterdam, The Netherlands, 1995; p. 563.
14. Tao, S.J. Positronium Annihilation in Molecular Substances. J. Chem. Phys. 1972, 56, 5499–5510.
15. Eldrup, M.; Lightbody, D.; Sherwood, N.J. The temperature dependence of positron lifetimes in solid pivalic acid. Chem. Phys. 1981, 63, 51.
16. Nakanishi, H.; Wang, S.J.; Jean, Y.C. Microscopic surface tension studied by positron annihilation. In Positron Annihilation Studies of Fluids; Sharma, S.C., Ed.; World Scientific: Singapore, 1988; p. 292.
17. Nakanishi, H.; Wang, Y.Y.; Jean, Y.C.; Sandreczki, T.C. Temperature and pressure dependences of free volume in an amine-cured epoxy polymer. In Positron Annihilation Studies of Fluids; Sharma, S.C., Ed.; World Scientific: Singapore, 1988; p. 285.
18. Han, X.; Chen, T.; Zhao, Y.; Gao, J.; Sang, Y.; Xiong, H.; Chen, Z. Relationship between the Microstructure and Performance of Graphene/Polyethylene Composites Investigated by Positron Annihilation Lifetime Spectroscopy. Nanomaterials 2021, 11, 2990.
19. Makarewicz, C.; Safandoska, M.; Idczak, R.; Rozanski, A. Positron annihilation lifetime spectroscopy analysis of plastic deformation of high-density polyethylene. Macromolecules 2021,

54, 9649–9662.

20. Lopez-Castanares, R.; Angeles, A.E.; Sanchez, V.; Fendler, J.H. Detection of glass transition in Poly(ethylene terephthalate) and Nylon-6 by positron annihilation. J. Appl. Polym. Sci. 1996, 62, 451–457.
21. Qi, N.; Chen, Z.Q.; Uedono, A. Molecular motion and relaxation below glass transition temperature in poly (methyl methacrylate) studied by positron annihilation. Rad. Phys. Chem. 2015, 108, 81–86.
22. Buttafava, A.; Consolati, G.; Mariani, M.; Quasso, F.; Ravasio, U. Effects induced by gamma irradiation of different polyesters studied by viscometry, thermal analysis and positron annihilation spectroscopy. Pol. Degr. Stab. 2005, 89, 133–139.
23. Bartos, J.; Bandzuch, P.; Sausa, O.; Kristiakova, K.; Kristiak, J.; Kanaya,T.; Jenninger, W. Free Volume Microstructure and Its Relationship to the Chain Dynamics in cis-1,4-Poly(butadiene) As Seen by Positron Annihilation Lifetime Spectroscopy. Macromolecules 1997, 30, 6906–6912.
24. Mostafa, M.; Ali, E.A.; Mohsen, M. Dynamic study of free volume properties in Polyethylene/Styrene Butadiene rubber blends by positron annihilation lifetime method. J. Appl. Polym. Sci. 2009, 113, 3228–3235.
25. Sui, H.; Liu, X.; Zhong, F.; Li, X.; Wang, B.; Ju, X. Polydimethylsiloxane rubber gamma radiation effect studies by positron annihilation lifetime spectroscopy. Rad. Eff. Defects Solids 2014, 169, 628–635.
26. Long, T.H.; Hieu, D.T.T.; Hao, L.H.; Cuong, N.T.; Loan, T.T.H.; Man, T.V.; Tap, T.D. Positron annihilation lifetime spectroscopy of Nafion and grafted-type polymer membranes for fuel cell applications. Polym. Eng. Sci. 2022, 62, 4005–4017.
27. Hamdy, F.M.M.; Abdel-Hady, E.E.; Salwa, S.M. Temperature dependence of the free volume in polytetrafluoroethylene studied by positron annihilation spectroscopy. Rad. Phys. Chem. 2007, 76, 160–164.
28. Consolati, G.; Genco, I.; Pegoraro, M.; Zanderighi, L. Positron annihilation lifetime (PAL) in Poly[1-(trimethyl-silyl)propine] (PTMSP): Free volume determination and time dependence of permeability. J. Polym. Sci. Part B Polym. Phys. 1996, 34, 357–367.
29. Coleman, G.P. Experimental techniques in positron spectroscopy. In Positron and Positronium Chemistry; Jean, Y.C., Mallon, P.E., Schrader, D.M., Eds.; World Scientific: Singapore, 2003; Chapter 3.
30. Saito, H.; Nagashima, Y.; Kurihara, T.; Hyodo, T. A new positron lifetime spectrometer using a fast-digital oscilloscope and BaF2 scintillators. Nucl. Instrum. Methods Phys. Res. Sect. A 2002, 487, 612–617.

31. Rytsölä, K.; Nissilä, J.; Kokkonen, J.; Laakso, A.; Aavikko, R.; Saarinen, K. Digital measurement of positron lifetime. Appl. Surf. Sci. 2002, 194, 260–263.
32. Becvar, F. Methodology of positron lifetime spectroscopy: Present status and perspectives. Nucl. Instrum. Methods Phys. Res. Sect. B 2007, 261, 871–874.
33. Ye, R.; Zhao, Q.H.; Wang, H.B.; Gu, B.C.; Pan, Z.W.; Liu, J.D.; Ye, B.J. Coincidence time resolution investigation of BaF2-based H6610 detectors for a digital positron annihilation lifetime Spectrometer. JINST 2020, 15, P06001.
34. Fang, M.; Bartholomew, N.; Di Fulvio, A. Positron annihilation lifetime spectroscopy using fast scintillators and digital Electronics. Nucl. Inst. Meth. Phys. Res. A 2019, 943, 162507.
35. Zhao, Q.H.; Ye, R.; Wang, H.B.; Cong, L.H.; Liu, J.D.; Zhang, H.J.; Ye, B.J. A multi-parameter discrimination digital positron annihilation lifetime spectrometer using a fast-digital oscilloscope. Nucl. Instrum. Meth. Phys. Res. A 2022, 1023, 165974.
36. Olsen, J.V.; Kirkegaard, P.; Pedersen, N.J.; Eldrup, M. PALSfit: A new program for the evaluation of positron lifetime spectra. Phys. Stat. Sol. 2007, 4, 4004–4006.
37. Gregory, R.B. Analysis of positron annihilation lifetime data by numerical Laplace inversion: Corrections for source terms and zero-time shift errors. Nucl. Instrum. Methods Phys. Res. Sect. A 1991, 302, 496–507.
38. Shukla, A.; Peter, M.; Hoffmann, L. Analysis of positron lifetime spectra using quantified maximum entropy and a general filter. Nucl. Instrum. Methods Phys. Res. Sect. A 1993, 335, 310–317.
39. 39. Kansy, J. Microcomputer program for analysis of positron annihilation lifetime spectra. Nucl. Instrum. Methods Phys. Res. Sect. A 1996, 374, 235–244.40. Consolati, G.; Nichetti, D.; Quasso, F. Probing the Free Volume in Polymers by means of Positron Annihilation Lifetime Spectroscopy. Polymers 2023, 15, 3128.
40. Consolati, G.; Nichetti, D.; Quasso, F. Probing the Free Volume in Polymers by means of Positron Annihilation Lifetime Spectroscopy. Polymers 2023, 15, 3128.
41. Yin, C.; Wang, L.; Li, J.; Zhou, Y.; Zhang, H.; Fang, P.; He, C. Positron annihilation characteristics, water uptake and proton conductivity of composite Nafion membranes. Phys. Chem. Chem. Phys 2017, 19, 15953.
42. Mohamed, H.F.M.; Abdel-Hady, E.E.; Abdel Hamed, M.O.; Said, M. Microstructure characterization of Nafion HP JP as a proton exchange membrane for fuel cell: Positron annihilation study. Acta Phys. Pol. A 2017, 132, 1543.
43. Elsharkawi, M.R.M.; Hassanien, M.H.M.; Mohamed, H.F.M.; Gomaa, M.M. Humidity effect on the transport properties on per-fluorinated sulfonic acid/PTFE proton exchange membranes: Positron annihilation study. Polym. Adv. Technol. 2022, 33, 952.

44. Awad, S.; Abdel-Hady, E.E.; Mohamed, H.F.M.; Elsharkawy, Y.S.; Gomaa, M.M.; Non-fluorinated PVA/SSA proton exchange membrane studied by positron annihilation technique for fuel cell applications. Polym. Adv. Technol. 2021, 32, 3322.
45. El-Gamal, S.; Elsayed, M. Positron annihilation and electrical studies on the influence of loading magnesia nanoribbons on PVA-PVP blend. Polym. Test. 2020, 89, 106681.
46. Wang, Z.; Yang, Y.; Peng, X.; Huang, Z.; Qian, L.; He, C.; Fang, P. Water diffusivity transition in fumed silica-filled polydimethylsiloxane composite: Correlation with the interfacial free volumes characterized by positron annihilation lifetime spectroscopy. J. Mater. Sci. 2021, 56, 3095.
47. Uedono, A.; Sako, K.; Ueno, W.; Kimura, M. Free volumes introduced by fractures of CFRP probed using positron annihilation. Compos. Part A 2019, 122, 54.
48. Winberg, P.; Eldrup, M.; Maurer, F.H.J. Nanoscopic properties of silica filled polydimethylsiloxane by means of positron annihilation lifetime spectroscopy. Polymer 2004, 45, 8253–8264.
49. Sharma, S.K.; Prakash, J.; Pujari, P.K. Effects of the molecular level dispersion of graphene oxide on the free volume characteristics of poly(vinyl alcohol) and its impact on the thermal and mechanical properties of their nanocomposites. Phys. Chem. Chem. Phys.2015, 17, 29201–29209.
50. Aly, H. Positron annihilation study on nickel and iron nanoparticles in natural rubber nanocomposites. Am. J. Appl. Sci. 2011, 8, 147–155.
51. Awad, S.; Chen, H.; Chen, G.; Gu, X.; Lee, J.L.; Abdel-Hady, E.E.; Jean, Y.C. Free volumes, glass transitions, and cross-links in zinc oxide/waterborne polyurethane nanocomposites. Macromolecules 2011, 44, 29–38.
52. Merkel, T.C.; Freeman, B.D.; Spontak, R.J.; He, Z.; Pinnau, I.; Meakin, P.; Hill, A.J. Ultrapermeable, reverse-selective nanocomposite membranes. Science 2002, 296, 519–522.
53. De Sitter, K.; Winberg, P.; D'Haen, J.; Dotremont, C.; Leysen, R.; Martens, J.A.; Mullens, S.; Maurer, F.H.J.; Vankelecom, I.F.J. Silica filled poly(1-trimethylsilyl-1-propyne) nanocomposite membranes: Relation between the transport of gases and structural characteristics. J. Membr. Sci. 2006, 278, 83–91.
54. Song, Q.; Nataraj, S.K.; Roussenova, M.V.; Tan, J.C.; Hughes, D.J.; Li, W.; Bourgoin, P.; Alam, M.A.; Cheetham, A.K.; Al-Muhtaseb, S.A.; et al. Zeolitic imidazolate framework (ZIF-8) based polymer nanocomposite membranes for gas separation. Energy Environ. Sci. 2012, 5, 8359–8369.
55. Sharma, S.K.; Pujari, P.K. Role of free volume characteristics of polymer matrix in bulk physical properties of polymer nanocomposites: A review of positron annihilation lifetime studies. Prog. Polym. Sci. 2017, 75, 31–47.

56. Liu, J.; Qi, N.; Zhou, B.; Chen, Z. Exceptionally High CO2 Capture in an Amorphous Polymer with Ultramicropores Studied by Positron Annihilation. ACS Appl. Mater. Interfaces 2019, 11, 30747.
57. Shantarovich, V.P.; Bekeshev, V.G.; Bermeshev, M.V.; Alentiev, D.A.; Gustov, V.W.; Belousova, E.V.; Kevdina, I.B.; Novikov, Y.A. Study of Microporosity of Polymer Glasses Using Techniques of Positron Annihilation and Low-Temperature Sorption of Carbon Dioxide. High Energy Chem. 2019, 53, 276.
58. Zhao, J.; Xu, M.; Shu, G.; Yang, Z.; Liu, Q.; Zeng, M.; Qi, C.; Cao, X.; Wang, B. Positron annihilation characteristics and catalytic performances of poly (vinyl alcohol) intercalated montmorillonite supported Pd0 nanoparticles composites. Rad. Phys. Chem. 2018, 153, 164.
59. Rhim, J.W.; Kuzeci, S.; Roy, S.; Akti, N.; Tav, C.; Yahsi, U. Effect of Free Volume on Curcumin Release from Various Polymer-Based Composite Films Analyzed Using Positron Annihilation Lifetime Spectroscopy. Materials 2021, 14, 5679.
60. Anbinder, P.S.; Macchi, C.; Amalvy, J.; Somoza, A. A study of the structural changes in a chitosan matrix produced by the adsorption of copper and chromium ions. Carbohydr. Polym. 2019, 222, 114987.
61. Nuruddin, M.; Chowdhury, R.A.; Lopez-Perez, N.; Montes, F.J.; Youngblood, J.P.; Howarter, J.A. Influence of Free Volume Determined by Positron Annihilation Lifetime Spectroscopy (PALS) on Gas Permeability of Cellulose Nanocrystal Films. Appl. Mater. Interfaces 2020, 12, 24380.
62. Shantarovich, V.P. On the role of free volume in pick-off annihilation and positronium chemical reactions. J. Radioanal. Nucl. Chem. 1996, 210, 357.
63. Wang, C.L.; Hirade, T.; Maurer, F.J.H.; Eldrup, M. Pedersen, N.J. Free-volume distribution and positronium formation in amorphous polymers: Temperature and positron-irradiation-time dependence. J. Chem. Phys. 1998, 108, 4654.
64. Biganeh, A.; Kakuee, O.; Rafi-Kheiri, H.; Lamehi-Rachti, M.; Sheikh, N.; Yahaghi, E. Positron Annihilation Lifetime and Doppler Broadening Spectroscopy of Polymers. Rad. Phys. Chem. 2020, 166, 108461.
65. Mogensen, O.E. Positron Annihilation in Chemistry; Goldanskii, V.I., Ed.; Springer Seires in Chemical Physics, vol. 58: Berlin/Heidelberg, Germany, New York, NY, USA, 1995.
66. Shantarovich, V.P. Positron annihilation and free volume studies in polymer glasses. J. Polym. Sci. Part B Polym. Phys. 2008, 46, 2485.
67. Srithawatpong, R.; Peng, Z.L.; Olson, B.G.; Jamieson, A.M.; Simha, R.; McGervey, J.D.; Maier, T.R.; Halasa, A.F.; Ishida, H. Positron annihilation lifetime studies of changes in free volume on cross-linking cis-polyisoprene, high-vinyl polybutadiene, and their miscible blends. J. Polym. Sci. Part B Polym. Phys. 1999, 37, 2754–2770.

68. Dlubek, G. Local Free-Volume Distribution from PALS and Dynamics of Polymers. In Polymer Physics. From Suspensions to Nanocomposites and Beyond; Utracki, L.A., Jamieson, A.M., Eds.; John Wiley & Sons: Singapore, 2010; pp. 421–472.
69. Simha, R.; Wilson, P.S. Thermal Expansion of Amorphous Polymers at Atmospheric Pressure. II. Theoretical Considerations. Macromolecules 1973, 6, 908.
70. Consolati, G.; Mossini, E.; Nichetti, D.; Quasso, F.; Viola, G.M.; Yaynik, E. Shape and Temperature Expansion of Free Volume Holes in Some Cured Polybutadiene-Polyisoprene Rubber Blends. Int. J. Mol. Sci. 2021, 22, 1436.
71. Utracki, L.A. Compressibility and thermal expansion coefficients of nanocomposites with amorphous and crystalline polymer matrix. Eur. Polym. J. 2009, 45, 1891–1903.
72. Consolati, G.; Quasso, F.; Simha, R.; Olson, G.B. On the relation between positron annihilation lifetime spectroscopy and lattice-hole-theory free volume. J. Pol. Sci. B 2005, 43, 2225–2229.
73. Consolati, G. On the Thermal Expansion of Nanohole Free Volume in Perfluoropolyethers. J. Phys. Chem. B 2005, 109, 10096–10099.
74. Consolati, G. Temperature dependence of nanoholes free volume in polypropylene glycols. Appl. Phys. Lett. 2006, 88, 111902.
75. Bradac, C.; Consolati, G.; Quasso, F. Temperature dependence of free volume in atactic polypropylene. Eur. Polym. J. 2009, 45, 3010–3015.
76. Consolati, G.; Mercurio, G.; Quasso, F. Free volume fraction and nanoholes shapes in polyvinyl acetate. Chem. Phys. Lett. 2009, 475, 54–57.
77. Consolati, G.; Nichetti, D.; Quasso, F. Constraints and Thermal Expansion of the Free Volume in a Micro-phase Separated Poly(ester-adipate)urethane. J. Polym. Sci. part B Polym. Phys. 2016, 54, 2104.
78. Consolati, G.; Nichetti, D.; Briatico Vangosa, F.; Quasso, F. Beyond the spherical approximation: Elongated free volume holes in rubbers: A positron annihilation study. Rubber Chem Technol. 2019, 92, 709–721.
79. Consolati, G.; Nichetti, D.; Quasso, F. Free volume expansion in some polybutadiene–acrylonitrile rubbers: Comparison between theory and experiments. Polym. Int. 2022, 71, 1287.
80. Olson, B.G.; Prodpran, T.; Jamieson, A.M.; Nazarenko, S. Positron annihilation in syndiotactic polystyrene containing α and β crystalline forms. Polymer 2002, 43, 6775–6784.
81. Wang, S.Q. On Chain Statistics and Entanglement of Flexible Linear Polymer Melts. Macromolecules 2007, 40, 8684–8694.

82. Milner, S.T. Predicting the Tube Diameter in Melts and Solutions. Macromolecules 2005, 38, 4929–4939.